Published in final edited form as:
J Membr Biol. 2014 October ; 247(0): 1043–1051. doi:10.1007/s00232-014-9682-8.

In Vivo Characterization of the Biodistribution Profile of Amphipol A8–35

A. Fernandez,
INSERM U1109, MN3t Lab, Labex Medalis, University of Strasbourg, 3 Avenue Molière, 67200 Strasbourg, France

C. Le Bon,
Laboratoire de Biologie Physico-Chimique des Protéines Membranaires, UMR 7099, Institut de Biologie Physico-Chimique (FRC 550), Centre National de la Recherche Scientifique/Université Paris 7, 13 Rue Pierre-et-Marie-Curie, 75005 Paris, France

N. Baumlin,
INSERM U1109, MN3t Lab, Labex Medalis, University of Strasbourg, 3 Avenue Molière, 67200 Strasbourg, France

F. Giusti,
Laboratoire de Biologie Physico-Chimique des Protéines Membranaires, UMR 7099, Institut de Biologie Physico-Chimique (FRC 550), Centre National de la Recherche Scientifique/Université Paris 7, 13 Rue Pierre-et-Marie-Curie, 75005 Paris, France

G. Crémel,
INSERM U1109, MN3t Lab, Labex Medalis, University of Strasbourg, 3 Avenue Molière, 67200 Strasbourg, France

J.-L. Popot, and
Laboratoire de Biologie Physico-Chimique des Protéines Membranaires, UMR 7099, Institut de Biologie Physico-Chimique (FRC 550), Centre National de la Recherche Scientifique/Université Paris 7, 13 Rue Pierre-et-Marie-Curie, 75005 Paris, France

D. Bagnard
INSERM U1109, MN3t Lab, Labex Medalis, University of Strasbourg, 3 Avenue Molière, 67200 Strasbourg, France

Abstract

Amphipols (APols) are polymeric surfactants that keep membrane proteins (MPs) water-soluble in the absence of detergent, while stabilizing them. They can be used to deliver MPs and other hydrophobic molecules in vivo for therapeutic purposes, e.g., vaccination or targeted delivery of drugs. The biodistribution and elimination of the best characterized APol, a polyacrylate derivative called A8–35, have been examined in mice, using two fluorescent APols, grafted with

bagnard@unistra.fr.

Research article submitted for publication in the special issue of *J. Membr. Biol*. on amphipols and their applications.

either Alexa Fluor 647 or rhodamine. Three of the most common injection routes have been used, intravenous (IV), intraperitoneal (IP), and subcutaneous (SC). The biodistribution has been studied by in vivo fluorescence imaging and by determining the concentration of fluorophore in the main organs. Free rhodamine was used as a control. Upon IV injection, A8–35 distributes rapidly throughout the organism and is found in most organs but the brain and spleen, before being slowly eliminated (10–20 days). A similar pattern is observed after IP injection, following a brief latency period during which the polymer remains confined to the peritoneal cavity. Upon SC injection, A8–35 remains essentially confined to the point of injection, from which it is only slowly released. An interesting observation is that A8–35 tends to accumulate in fat pads, suggesting that it could be used to deliver anti-obesity drugs.

Keywords

Membrane proteins; Surfactants; Polymers; Vectorization; Vaccination; Obesity

Introduction

Amphipols (APols) are polymeric surfactants that maintain membrane proteins (MPs) water-soluble in the absence of detergent, while stabilizing them (Popot et al. 2011; Zoonens and Popot 2014). Their physical–chemical properties make them as promising vehicles for the delivery of MPs, or, possibly, other therapeutic agents, such as hydrophobic membrane-targeting peptides (Nasarre et al. 2010). Previous studies have shown that A8–35, a polyacrylate-based APol (Tribet et al. 1996), is not toxic when added to cell cultures at a concentration sufficient to deliver MPs to their plasma membrane (Popot et al. 2003), or when injected to mice at doses sufficient to formulate a vaccine (Tifrea et al. 2011). A8–35 is non-immunogenic by itself (Popot et al. 2003), but, when used to trap a MP used as an immunogen, it potentiates the protection afforded to vaccinated animals (Tifrea et al. 2011, 2014). Above a very low critical aggregation concentration (~0.002 g L^{-}; Giusti et al. 2012), A8–35 self-associates into well-defined, ~40-kDa particles (Gohon et al. 2006). Its binding to MPs, albeit non-covalent, is very stable even at high dilution (Charvolin et al. 2009; Tribet et al. 1997, 2009; Zoonens et al. 2007), as inevitably happens when injecting MP/APol complexes into humans or animals. This, as well as its stabilizing effect, may contribute to the higher efficacy of vaccines formulated with APols rather than detergents (Tifrea et al. 2011, 2014).

Our previous work on COS cells revealed the stable integration of a fluorescent, NBD-labeled version of A8–35 ($FAPol_{NBD}$) in the cell membrane up to 96 h before internalization and lysosomal degradation. When $FAPol_{NBD}$ was injected in tumor-bearing mice by the intraperitoneal (IP) route, a fluorescent signal was detected in blood vessels vascularizing the tumors and deep into the adjacent tissue (Popot et al. 2011). This suggested that APols exhibit good biodistribution profiles. However, nothing is known about their long-term behavior in animals, and systematic biodistribution profiles have not been established yet. Here, we report the distribution profiles of two fluorescent versions of A8–35 carrying, respectively, the far-red fluorophore Alexa Fluor 647 ($FAPol_{AF647}$) or the red fluorophore rhodamine ($FAPol_{rhod}$). Profiles were obtained 4 h to 20 days post-injection through three

different routes: intravenous (IV), IP, and subcutaneous (SC). While confirming the good biodistribution of APols, this study reveals an interesting site-specific behavior of A8–35, opening the way to unexpected applications for long-term local delivery of MPs or other hydrophobic therapeutic agents (Nasarre et al. 2010).

Materials and Methods

Materials and Instrumentation

Poly-acrylic acid, ammonium formate, triethylamine (TEA), dicyclohexylcarbodiimide, octylamine, and isopropylamine were from Sigma-Aldrich. Methanol, dimethylformamide (DMF), and *N*-methylpyrrolidone were from SDS. Palladium on activated charcoal, sodium methoxide, 1-hydroxybenzotriazole, and Celite were from Acros. AF647 carboxylic acid succinimydyl ester (AF647-NHS) was from Life Technologies. A8–35 was synthesized according to the procedure described in Gohon et al. (2004, 2006). UV–visible spectroscopy measurements were carried out on a HP-8453 UV–VIS spectrometer (Agilent Technologies). Fluorescence spectroscopy was performed on a PTI fluorescence spectrometer (Serlabo Technologies) controlled by Felix software. NMR spectroscopyexperiments were performed on a Bruker Avance 400 MHz instrument (Bruker, Wissembourg, France).

Synthesis and Purification of AF647- and Rhodamine-Labeled A8–35

AF647-labeled A8–35 ($FAPol_{AF647}$) was obtained by grafting AF647 carboxylic acid succinimydyl ester (AF647-NHS) onto the amine moiety carried by an amino-prefunctionalized A8–35 (UAPol-NH_2), whose synthesis has been described elsewhere (Zoonens et al. 2007) (Fig. 1). UAPol-NH_2 was reacted with AF647-NHS according to the following procedure. 80.3 mg (18.67 μmol) of UAPol-NH_2 was dissolved in 6 mL of DMF under magnetic stirring at 40 °C. 5 mg (3.85 μmol) of AF647-NHS was dissolved in 250 μL of DMF, and 5 μL of TEA (as a basic activator) was added to the reaction medium. The temperature was lowered to 30 °C overnight. The reaction medium was protected from light. The solution was purified by three cycles of precipitation at acidic pH (5 % sodium phosphate, pH 2)/centrifugation/dissolution at basic pH (1 M borate, pH 8), as described in Gohon et al. (2004, 2006). The FAPol solution was filtrated on a 0.22-μm acetate filter, dialyzed against water with Spectra Por 7 membrane (cut-off 2 kDa) and freeze-dried. To further separate $FAPol_{AF647}$ from a secondary product, the crude FAPol was purified by size exclusion chromatography (SEC) on an HR Superose 12 16/50 column in a buffer containing 20 mM Tris/HCl, pH 8, and 100 mM NaCl. Finally, the solution was dialyzed against water and freeze-dried, yielding 50 mg (yield ~60 % with respect to UAPol-NH_2) of purified $FAPol_{AF647}$ as a turquoise-blue powder.

Rhodamine-grafted A8–35 ($FAPol_{rhod}$) was synthesized as described in Giusti et al. (2012).

Chemical Composition of $FAPol_{AF647}$

The chemical composition of $FAPol_{AF647}$ was characterized by ^{1}H and ^{13}C NMR spectroscopy of its UAPol precursor (content of octyl- and isopropylamine) and by spectrophotometry (amount of AF647 grafted; cf. Fig. 2c). UAPol contains 2.6 % of amino

linker, corresponding to ~8 amine functions per 40-kDa particle. The grafting ratio of AF647 is ~0.3 %, or ~1 fluorophore per particle.

Solution Behavior of $FAPol_{AF647}$

The solution behavior of $FAPol_{AF647}$ was characterized by SEC performed on anÄ$_{kta}$ Purifier 10 FPLC system (GE Healthcare) equipped with a Superose 12 10/300 GL column. Detection was performed at 220 and 650 nm. Elution buffer was 20 mM Tris/HCl, pH 8, 100 mM NaCl. The elution flow rate was 0.5 mL min^{-} and the injected polymer concentration 5 g L^{-} (Fig. 2a, b). The absorption spectrum of $FAPol_{AF647}$ was recorded on a 0.1-g L^{-} solution in 20 mM Tris/HCl, pH 8 (Fig. 2c) and the fluorescence emission and excitation spectra on a 0.001-g L^{-} $FAPol_{AF647}$ solution in the same buffer (Fig. 2d). The absorption and fluorescence spectra of $FAPol_{rhod}$ are shown in Giusti et al. (2012).

Preparation of Solutions

$FAPol_{AF647}$, $FAPol_{rhod}$, and free rhodamine were prepared as stock solutions of 5 g L^{-} in ultra-pure water and diluted to 0.1 g L^{-} with PBS before injection.

Whole-Body In Vivo Biodistribution

18 female NMRI Nude 10-week-old mice (two per injection mode) were subjected to IP, SC, or IV retro-orbital sinus injections of 100 μL of $FAPol_{AF647}$, $FAPol_{rhod}$, or free rhodamine solutions, corresponding to 10 μg of products. Fluorescence was detected on gas-anesthetized animals, thanks to a Bioimager (Nightowl LB-983, Berthold), as previously described (Destouches et al. 2011; Page et al. 2011). The fluorescence was measured for each animal from the ventral and the dorsal sides at t_0 (before injection), 10 min, 1 h, 4 h, 24 h, 48 h, 72 h, 10 days, and 20 days. Acquisitions were performed during 30 s for IP and IV injections and 1 s for SC injections.

Ex Vivo Biodistribution

30 female Balb/C 10-week-old mice were subjected to IP, SC, or IV retro-orbital sinus injections (two animals per injection mode) with 100 μL of $FAPol_{AF647}$ solution. Two mice of each group were sacrificed at 4 h, 24 h, 72 h, 10 days, and 20 days after injection and dissected in order to collect organs (liver, kidney, spleen, fat pads, heart, lungs, and brain). Acquisitions were performed during 1 s.

Data Analysis

All images were collected and analyzed using the Night-Owl 2 software. Images and quantitative signals were exported to Excel and GraphPad for data analysis and graphic representations.

Results

Synthesis and Solution Behavior of $FAPol_{AF647}$

$FAPol_{AF647}$ was synthesized following the same route as used previously for the synthesis of $FAPol_{NBD}$ (Zoonens et al. 2007), namely by grafting a derivative of the fluorophore onto

an amino arm carried by a functionalized A8–35 (Fig. 1; see “Materials and Methods” section). It was purified by repeated cycles of precipitation at acidic pH and re-dissolution at basic pH, followed by SEC. As classically observed for APols grafted with small ligands (Zoonens et al. 2007; Le Bon et al. 2014), the solution behavior of $FAPol_{AF647}$, examined by SEC (Fig. 2), was identical to that of ungrafted A8–35, namely self-association into ~40-kDa globular particles (Gohon et al. 2006), the purified polymer comprising ~1 fluorophore per particle. $FAPol_{AF647}$ presents an absorption maximum at 651 nm (Fig. 2c, d) and an emission maximum at 668 nm (Fig. 2d). The crude product not only contains a majority of AF647-grafted APol particles, but also a small fraction (~25 % w/w) of much smaller objects, probably small polymers that are not hydrophobic enough to associate into particles but are strongly labeled (Fig. 2a). These contaminants were removed by SEC and are absent in purified $FAPol_{AF647}$ (Fig. 2b).

Biodistribution of $FAPol_{AF647}$

Following IV Injection

IV injection is one of the most common routes of administration and is considered to give the best bioavailability. Indeed, following injection of $FAPol_{AF647}$ in the retro-orbital sinus, the fluorescent signal propagated rapidly throughout the whole body of the animals (Fig. 3). Strikingly, the signal was extremely stable, profiles obtained 10 min post-injection being similar to those obtained at 72 h. A significant decrease was first seen at 10 days post-injection. Ventral views of the animals revealed, as expected from IV injection, a rapid concentration in the liver. This hepatic signal was clearly detectable up to 72 h, with a maximal intensity seen at 4 h. The concentration of the signal in the liver was confirmed when collecting organs at different time-points in some of the animals. As seen in Fig. 3, 94 % of the signal was measured in the liver, the rest being distributed among the lungs (3.3 %), the heart (0.6 %), and the kidneys (2.1 %), the latter signal being consistent with an excretion process. Interestingly, there was no detectable signal in the spleen or in the brain. Since all organs (except liver) were negative at 24 h when removed from the body, the observed fluorescent signal in the whole body at this time-point is mainly due to the persistence of APols in the circulation.

Biodistribution of $FAPol_{AF647}$ Following IP Injection

IP injections are widely used in animal studies because of the ease of the procedure. Following injection of $FAPol_{AF647}$, the fluorescent signal remained concentrated in the peritoneal cavity for ~1 h (Fig. 4). It then reached the circulation to produce a uniform signal in the body, concomitant with a persistent and intense staining of the liver for up to 72 h. As for the IV route, the signal progressively disappeared at 10 and 20 days post-injection, confirming the slow release of APols from the body. The collection of organs at different time-points showed a large amount of signal in abdominal fat pads (45 %) and in the liver (55 %) up to 72 h. With the exception of a faint signal in the liver, signals were barely undetectable at 10 and 20 days, suggesting complete elimination. In all cases, no signal was observed in the lung, heart, spleen, and brain, implying no accumulation of APols in these tissues. A very modest signal in kidneys presumably reflected renal elimination. It was difficult to monitor due to the slow release from fat and liver, generating very low doses of

APol to eliminate at any given time point. Hence, as for the IV route, a majority of APols remains circulating once diffusing from fat and is progressively eliminated, presumably via the hepatic route.

Biodistribution of $FAPol_{AF647}$ Following SC Injection

The SC route is known to lead to slow but complete absorption of drugs. Indeed, following injection of the $FAPol_{AF647}$ bolus, a compact and restricted signal was observed at the injection site for the entire period of analysis (Fig. 5). The intensity of the spot decreased very slowly, but was still detectable after 20 days. This high site-specific concentration effect impeded detection of APols in the rest of the body, including at the ventral view. Consistently, fluorescence was found associated with the dorsal fat pads, which appear to be a very efficient natural reservoir for APols. With the exception of the liver, which showed significant staining, suggesting hepatic elimination of APols, and hence, diffusion from the injection site, APols could not be detected in any of the collected organs, due to their low circulating concentration.

Biodistribution of a Rhodamine-Labeled APol

To validate the biodistribution profiles, experiments were repeated using a rhodamine-labeled version of A8–35 ($FAPol_{rhod}$; see Giusti et al. 2012). As seen in Fig. 6, distribution profiles fully matched those obtained for $FAPol_{AF647}$. The profiles are presented for each adminis tration route with the corresponding distribution of free rhodamine, which served as a control experiment. This confirmed that the observed persistent signals do correspond to $FAPol_{rhod}$, given that the signal of the free dye (although ~100× concentrated compared to the label carried by $FAPol_{rhod}$) reaches a peak around 1 h and is almost gone at 72 h. Free rhodamine was detectable in urine 1–4 h post-injection using a plate reader (Tristar II, Berthold; *not shown*). In all cases, $FAPol_{rhod}$ remained undetectable in spite of a detection sensitivity compatible with the measure of 1,000× less $FAPol_{rhod}$-containing solution than the one being injected (*data not shown*). This is consistent with very slow release of $FAPol_{rhod}$, generating fluorescent signal intensity below the detection threshold.

Discussion

The present study was designed to visualize the distribution profiles of fluorescent versions of APols. This was motivated by the results of previous studies (Popot et al. 2011; Tifrea et al. 2011, 2014) demonstrating that APols can be used in vivo as vehicles for MPs or hydrophobic therapeutic agents. The systematic evaluation of three of the major administration routes (IV, IP, SC) revealed that APol A8–35 exhibits a long-lasting distribution in the whole body circulation up to 10–20 days. It also showed that fat pads can trap APols, which are subsequently slowly released over time.

Following administration of FAPols using the IV route, a rapid and broad diffusion of the fluorescent signal was observed, consistent with efficient circulation of APols in the blood flow. The hepatic signal seen 10 min post-injection is consistent with the detoxification function of this organ. The fluorescent signals in the liver parenchyma were clearly confirmed when imaging dissected organs, whereas most of the other organs were not

fluorescent. This suggested that the majority of the detectable FAPols remains in blood circulation. However, because low doses of FAPols were used, and given limitations to the sensitivity of the imaging system, it cannot be excluded that a fraction of FAPols can exit the blood flow to enter organs. This is indeed seen at the histologic level when using a higher concentration of FAPol (1 mg L^{-}_{NBD}) in tumor-bearing mice in which vascularized tumors had strong APol signals distant from the blood flow (Popot et al. 2011). The persistent signal in the blood flow suggests that APols can interact with serum lipoproteins and/or the membranes of circulating red and white cells. From the control experiments performed with rhodamine, one can conclude that the observed distributions correspond to intact FAPols, and not to cleaved fluorescent dye, because, as expected, free rhodamine is rapidly eliminated from the body. To our knowledge, there is very few if any report of detergent or detergent-like compounds biodistribution using in vivo live imaging. This renders difficult any comparison with our study on APols with other drug vehicles. The closest situation is certainly the case of liposomes, exosomes, and/or microvesicles (EV) that share some of the biochemical properties of APols. Indeed, a very recent study of Lai et al. (2014) provided in vivo data nicely and precisely detailing the tissue distribution of luminescent EVs. This revealed that the EVs first undergo a rapid distribution phase followed by a longer elimination phase via hepatic and renal routes within 6 h. Particular EVs retention was observed in hepatic and renal or tumor tissues similar to our description of IV injections of APols here or as previously described (Popot et al. 2011). Hence, the distribution profile obtained with SC injection of APols is quite unique and we were not able to find reports of similar activity. Future experiments will use single photon emission computed tomography imaging using gamma- emitting radioisotope-coupled APols to obtain pharmaco-kinetic data in a more quantitative and sensitive manner (Ding and Wu 2012). Additionally, it would be interesting to analyze the biodistribution profile of orally administrated APols because this route is still the preferred route of administration of drugs. However, transdermal delivery may also represent an exquisite approach because this administration route is circumventing two of the most important disadvantages of other routes by reducing first-pass metabolism associated with oral delivery and is less painful than injections. This is particularly interesting in the context of vaccine (Schoellhammer et al. 2014) which is indeed a clear and already validated indication for the use of APols (Tifrea et al. 2014).

When using IP or SC routes, long-term body retention of FAPols was also observed. Fat pads, in particular, were found to trap FAPols that were slowly released from the injection sites. This intriguing property may reflect the amphipathic nature of APols, which may find in lipophilic areas a natural reservoir. This unforeseen result opens interesting opportunities to use APols for the delivery of anti-obesity drugs such as CLA (conjugated linoleic acid; see Blankson et al. 2000). Indeed, recent work has shown that nano-emulsions enhanced the bioavailability of CLA and its anti-obesity effect (Kim et al. 2013). The stable localization observed under the skin also suggests the interesting possibility of using APols for long-term and slow release of drugs. This is in turn opening the possibility to extend the use of APols for the delivery of hydrophobic drugs in the context of the several chronic diseases requiring long-term delivery of drugs such as chronic pain, psychiatric disorders, hypertensive diseases, HIV, or cancer.

As a conclusion, the biodistribution profile of APols is compatible with several in vivo applications. Depending on the administration route, APol-associated MPs or drugs can be delivered in a long-term manner, eventually benefitting from natural reservoirs such as fat. One may also note that, because it is possible to functionalize APols with essentially any desirable molecule (Le Bon et al. 2014), targeting MPs, peptides, or drugs to selected organs using APols tagged with organ-specific ligands is a realistic proposition.

Acknowledgments

This work has been carried out within the LABEX ANR-10-LABX-0034 Medalis and received a financial support from French Government managed by “Agence National de la Recherche” under “Programme d'investissement d'avenir” and Fondation pour la Recherche Médicale (FRM/Rotary International), the French Centre National de la Recherche Scientifique, University Paris-7, U.S. National Grant R01AI092129 from the National Institute of Allergy and Infectious Diseases, French Agence Nationale pour la Recherche Grant “X-Or”, ANR SVSE5 2010-BLAN-1535, and Grant “DYNAMO”, ANR-11-LABX-0011-01 from the French “Initiative d'Excellence” Program.

References

Blankson H, Stakkestad JA, Fagertun H, Thom E, Wadstein J, Gudmundsen O. Conjugated linoleic acid reduces body fat mass in overweight and obese humans. J Nutr. 2000; 130:2943–2948. [PubMed: 11110851]

Charvolin D, Perez J-B, Rouvière F, Giusti F, Bazzacco P, Abdine A, Rappaport F, Martinez KL, Popot J-L. The use of amphipols as universal molecular adapters to immobilize membrane proteins onto solid supports. Proc Natl Acad Sci USA. 2009; 106:405–410. [PubMed: 19116278]

Destouches D, Page N, Hamma-Kourbali Y, Machi V, Chaloin O, Frechault S, Birmpas C, Katsoris P, Beyrath J, Albanese P, Maurer M, Carpentier G, Strub J-M, Van Dorsselaer A, Muller S, Bagnard D, Briand JP, Courty J. A simple approach to cancer therapy afforded by multivalent pseudopeptides that target cell-surface nucleoproteins. Cancer Res. 2011; 71:3296–3305. [PubMed: 21415166]

Ding H, Wu F. Image guided biodistribution and pharmaco-kinetic studies of theranostics. Theranostics. 2012; 2:1040–1053. [PubMed: 23227121]

Giusti F, Popot J-L, Tribet C. Well-defined critical association concentration and rapid adsorption at the air/water interface of a short amphiphilic polymer, amphipol A8–35: a study by Förster resonance energy transfer and dynamic surface tension measurements. Langmuir. 2012; 28:10372–10380. [PubMed: 22712750]

Gohon Y, Pavlov G, Timmins P, Tribet C, Popot J-L, Ebel C. Partial specific volume and solvent interactions of amphipol A8–35. Anal Biochem. 2004; 334:318–334. [PubMed: 15494140]

Gohon Y, Giusti F, Prata C, Charvolin D, Timmins P, Ebel C, Tribet C, Popot J-L. Well-defined nanoparticles formed by hydrophobic assembly of a short and polydisperse random terpolymer, amphipol A8–35. Langmuir. 2006; 22:1281–1290. [PubMed: 16430295]

Kim D, Park J-H, Kweon D-J, Han GD. Bioavailability of nanoemulsified conjugated linoleic acid for an antiobesity effect. Int J Nanomed. 2013; 8:451–459.

Lai CP, Mardini O, Ericsson M, Prabhakar S, Maguire CA, Chen JW, Tannous BA, Breakefield XO. Dynamic biodistribution of extracellular vesicles in vivo using a multimodal imaging reporter. ACS Nano. 2014; 8:483–594. [PubMed: 24383518]

Le Bon C, Popot J-L, Giusti F. Labeling and functionalizing amphipols for biological applications. J Membr Biol. 2014 doi:10. 1007/s00232-014-9655-y.

Nasarre C, Roth M, Jacob L, Roth L, Koncina E, Thien A, Labourdette G, Poulet P, Hubert P, Crémel G, Roussel G, Aunis D, Bagnard D. Peptide-based interference of the trans-membrane domain of neuropilin-1 inhibits glioma growth in vivo. Oncogene. 2010; 29:2381–2392. [PubMed: 20140015]

Page N, Gros F, Schall N, Décossas M, Bagnard D, Briand J-P, Muller S. HSC70 blockade by the therapeutic peptide P140 affects autophagic processes and endogenous MHCII presentation in murine lupus. Ann Rheum Dis. 2011; 70:837–843. [PubMed: 21173017]

Popot J-L, Berry EA, Charvolin D, Creuzenet C, Ebel C, Engelman DM, Flötenmeyer M, Giusti F, Gohon Y, Hervé P, Hong Q, Lakey JH, Leonard K, Shuman HA, Timmins P, Warschawski DE, Zito F, Zoonens M, Pucci B, Tribet C. Amphipols: polymeric surfactants for membrane biology research. Cell Mol Life Sci. 2003; 60:1559–1574. [PubMed: 14513831]

Popot J-L, Althoff T, Bagnard D, Banères J-L, Bazzacco P, Billon-Denis E, Catoire LJ, Champeil P, Charvolin D, Cocco MJ, Crémel G, Dahmane T, de la Maza LM, Ebel C, Gabel F, Giusti F, Gohon Y, Goormaghtigh E, Guittet E, Kleinschmidt JH, Kühlbrandt W, Le Bon C, Martinez KL, Picard M, Pucci B, Rappaport F, Sachs JN, Tribet C, van Heijenoort C, Wien F, Zito F, Zoonens M. Amphipols from A to Z. Annu Rev Biophys. 2011; 40:379–408. [PubMed: 21545287]

Schoellhammer CM, Blankschtein D, Langer R. Skin permeabilization for transdermal drug delivery: recent advances and future prospects. Expert Opin Drug Deliv. 2014; 11:393–407. [PubMed: 24392787]

Tifrea DF, Sun G, Pal S, Zardeneta G, Cocco MJ, Popot J-L, de la Maza LM. Amphipols stabilize the Chlamydia major outer membrane protein and enhance its protective ability as a vaccine. Vaccine. 2011; 29:4623–4631. [PubMed: 21550371]

Tifrea D, Pal S, Cocco MJ, Popot J-L, de la Maza LM. Increased immuno accessibility of MOMP epitopes in a vaccine formulated with amphipols may account for the very robust protection elicited against a vaginal challenge with C. muridarum. J Immunol. 2014; 192(11):5201–5213. [PubMed: 24778450]

Tribet C, Audebert R, Popot J-L. Amphipols: polymers that keep membrane proteins soluble in aqueous solutions. Proc Natl Acad Sci USA. 1996; 93:15047–15050. [PubMed: 8986761]

Tribet C, Audebert R, Popot J-L. Stabilization of hydrophobic colloidal dispersions in water with amphiphilic polymers: application to integral membrane proteins. Langmuir. 1997; 13:5570–5576.

Tribet C, Diab C, Dahmane T, Zoonens M, Popot J-L, Winnik FM. Thermodynamic characterization of the exchange of detergents and amphipols at the surfaces of integral membrane proteins. Langmuir. 2009; 25:12623–12634. [PubMed: 19594168]

Zoonens M, Popot J-L. Amphipols for each season. J Membrane Biol. 2014 doi:10.1007/s00232-014-9666-8.

Zoonens M, Giusti F, Zito F, Popot J-L. Dynamics of membrane protein/amphipol association studied by Förster resonance energy transfer. Implications for in vitro studies of amphipol-stabilized membrane proteins. Biochemistry. 2007; 46:10392–10404. [PubMed: 17705558]

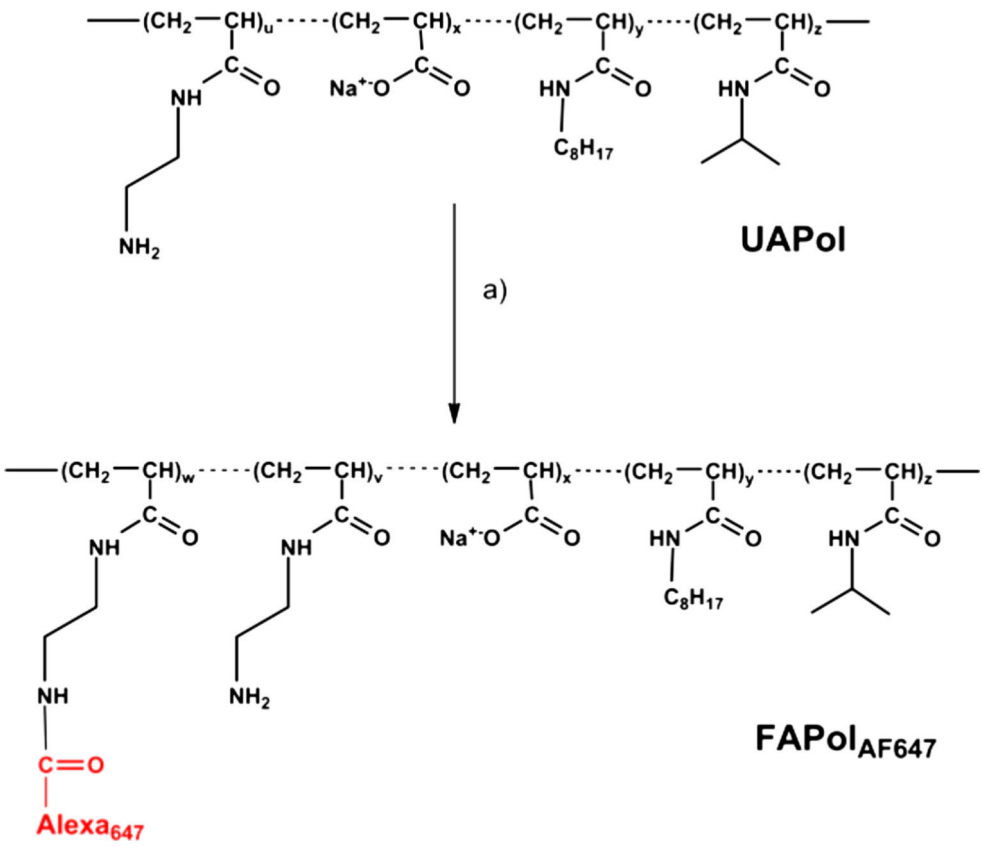

Fig. 1.

Synthesis of FAPol$_{AF647}$ by functionalization of UAPol-NH$_2$. (*a*) AF647-NHS, DMF, TEA (cat.), 40 °C, 12 h, yielding FAPol$_{AF647}$. Chemical compositions: UAPol-NH$_2$: x ≈ 32.4 %, y ≈ 25 %, z ≈ 40 %, u ≈ 2.6 %; FAPol$_{AF647}$: x ≈ 32.4 %, y ≈ 25 %, z ≈ 40 %, v ≈ 2.3 %, and w ≈ 0.3 %

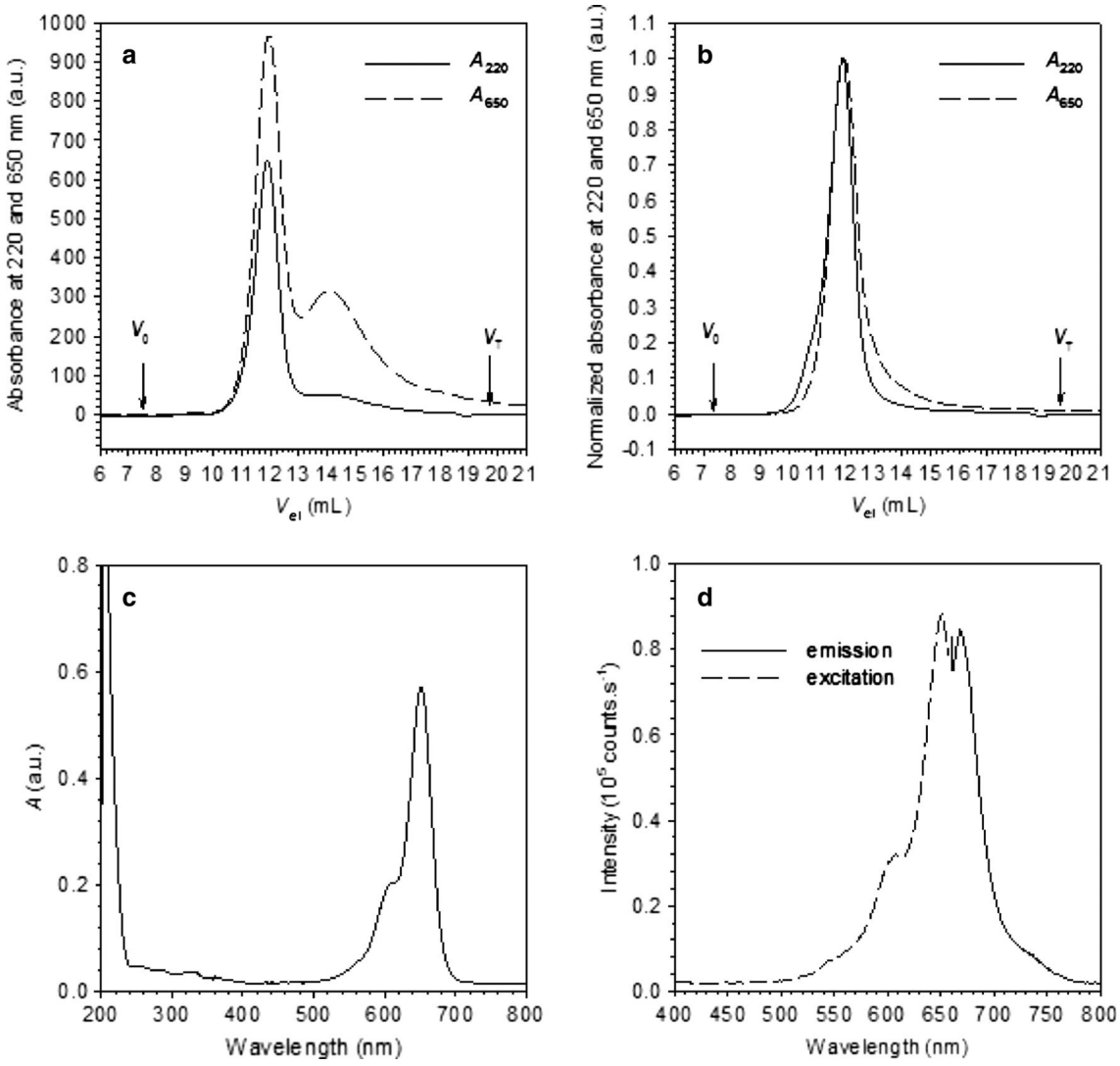

Fig. 2.

Solution and spectroscopic properties of $FAPol_{AF647}$. **a** Elution profiles at 220 nm (*solid line*) and 650 nm (*dashed line*) of crude $FAPol_{AF647}$. The concentration injected was 5 g L^{-}. Elution buffer: 0.1 M NaCl, 20 mM Tris/HCl, pH 8. *au* arbitrary units, V_{el} elution volume, V_0 excluded volume, V_T total volume. **b** Elution profiles at 220 nm (*solid line*) and 650 nm (*dashed line*) of purified $FAPol_{AF647}$. Same conditions. The profiles were normalized to the same maximum. **c** Absorption spectrum of 0.1 g L^{-} $FAPol_{AF647}$ in the same buffer. **d** Emission (*solid line*) and excitation (*dashed line*) spectra of a 0.001 g L^{-} solution of purified $FAPol_{AF647}$; same buffer

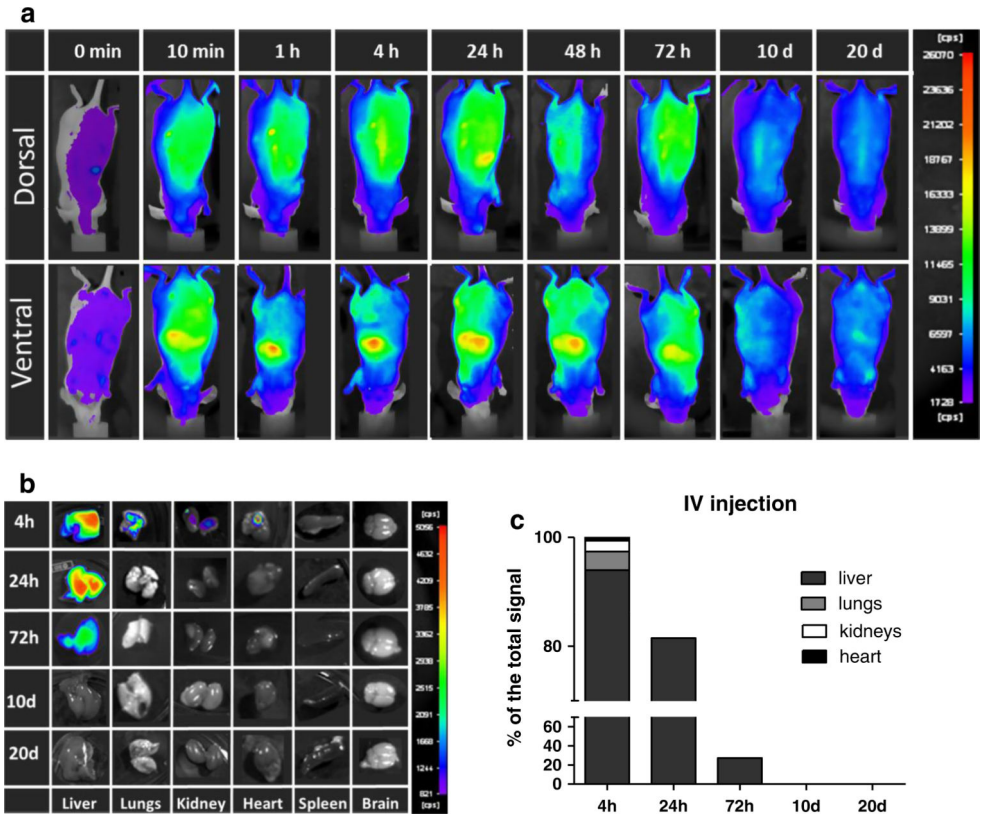

Fig. 3.

Biodistribution of $FAPol_{AF647}$ following intravenous injection. **a** Time-series images of a representative animal before and after intravenous injection of 10 μg $FAPol_{AF647}$. *Upper row* dorsal view, *lower row* ventral view. **b** Time-series images of organs collected at different time-points. **c** Quantitation of fluorescent signals measured in organs over time

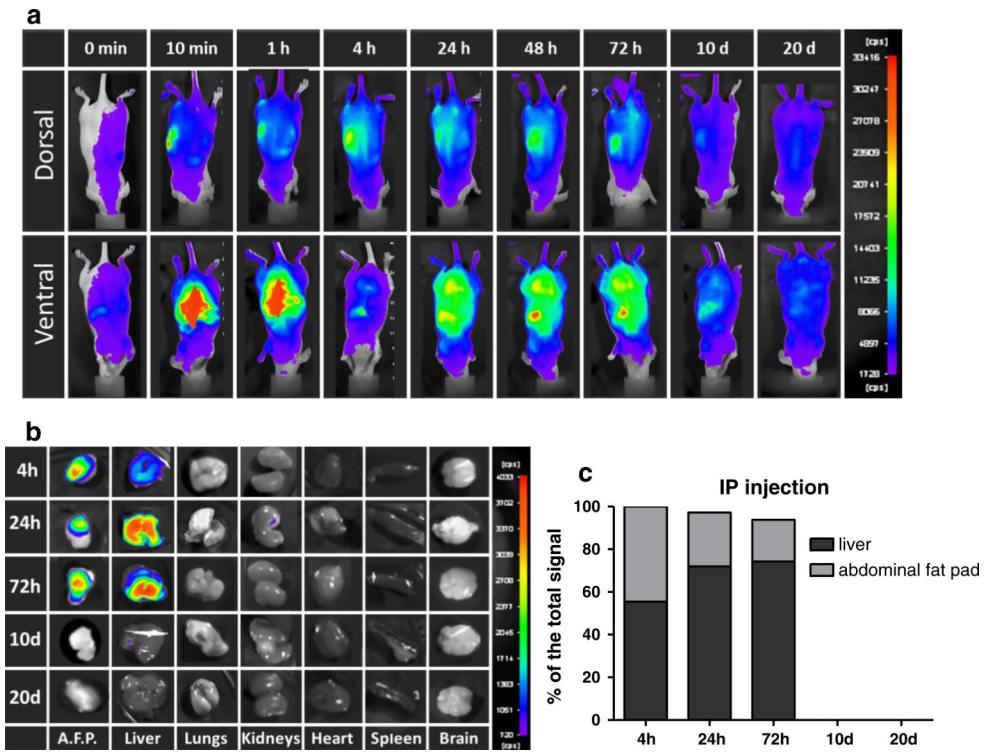

Fig. 4.

Biodistribution of $FAPol_{AF647}$ following intraperitoneal injection. **a** Time-series images of a representative animal before and after intraperitoneal injection of 10 μg $FAPol_{AF647}$. *Upper row* dorsal view, *lower row* ventral view. **b** Time-series images of organs collected at different time-points. **c** Quantitation of fluorescent signals measured in organs over time

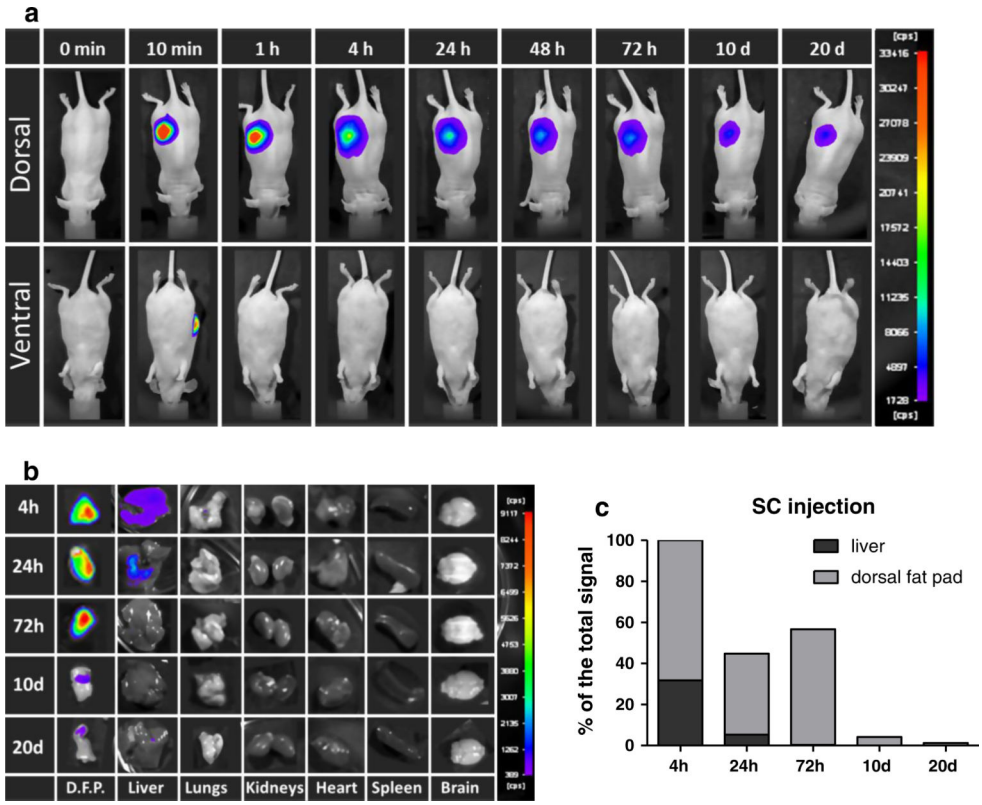

Fig. 5.

Biodistribution of $FAPol_{AF647}$ following subcutaneous injection. **a** Time-series images of a representative animal before and after subcutaneous injection of 10 μg $FAPol_{AF647}$. *Upper row* dorsal view, *lower row* ventral view. **b** Time-series images of organs collected at different time-points. **c** Quantitation of fluorescent signals measured in organs over time

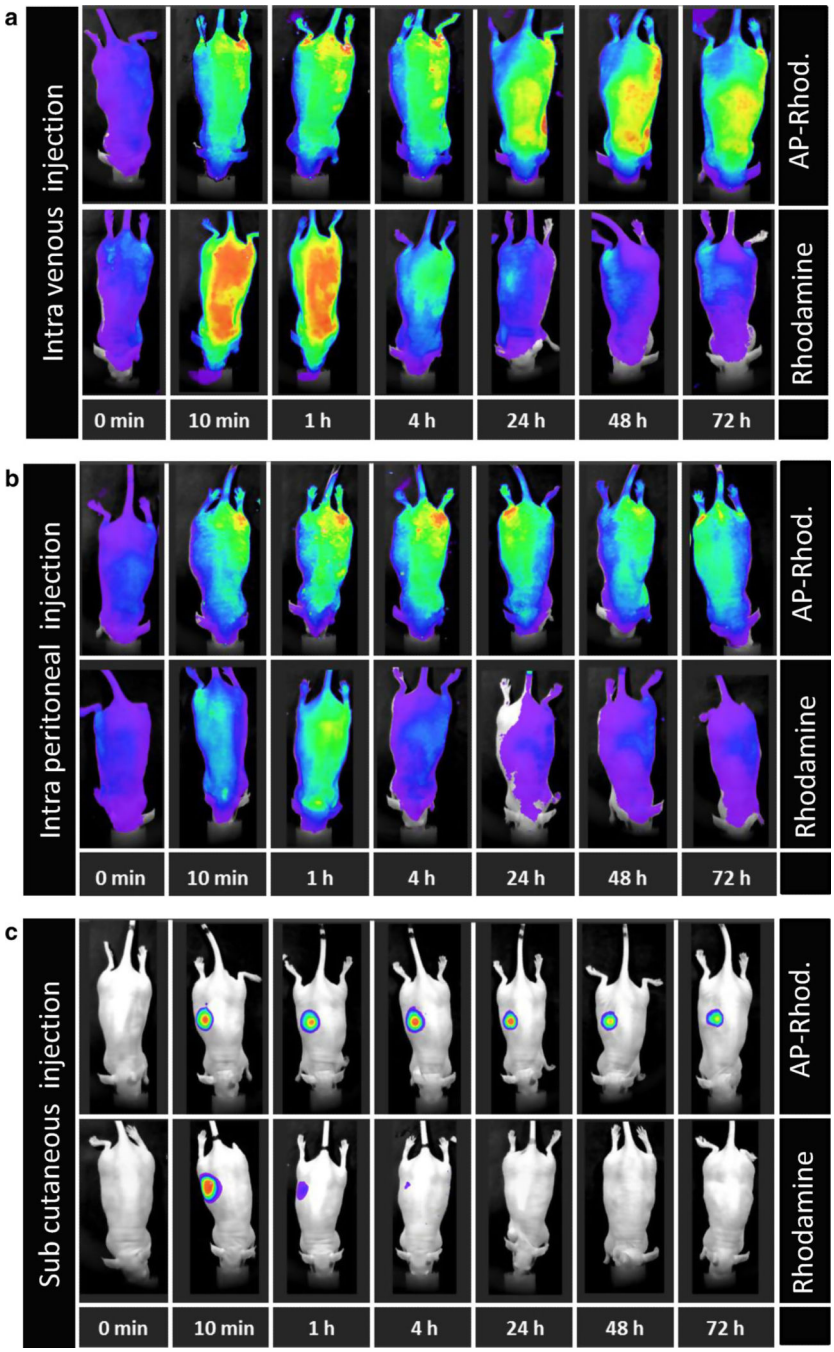

Fig. 6.

Biodistribution of $FAPol_{rhod}$. Dorsal view time-series images of representative animals receiving a an intravenous injection of 10 μg $FAPol_{rhod}$ (*upper row*) or 10 μg free rhodamine (*lower row*), b an intraperitoneal injection of 10 μg $FAPol_{rhod}$ (*upper row*) or 10 μg free rhodamine (*lower row*), or c a subcutaneous injection of 10 μg $FAPol_{rhod}$ (*upper row*) or 10 μg free rhodamine (*lower row*)